



An interplay between beam–beam and beam coupling impedance effects in the Future Circular e^+e^- Collider

M. Migliorati^{1,a} , E. Carideo^{1,2}, D. De Arcangelis¹, Y. Zhang³, M. Zobov⁴

¹ University of Rome ‘La Sapienza’ and INFN Sezione Roma1, 00185 Rome, Italy

² CERN, 1217 Meyrin, Geneva, Switzerland

³ Institute of High Energy Physics, Beijing 100049, China

⁴ INFN - LNF, Frascati, 00044 Rome, Italy

Received: 24 May 2021 / Accepted: 15 November 2021

© The Author(s), under exclusive licence to Società Italiana di Fisica and Springer-Verlag GmbH Germany, part of Springer Nature 2021

Abstract In order to reach high luminosity, the Future Circular e^+e^- Collider will need very intense beams with small emittances and small beta functions in the interaction points. This is achieved with a large Piwinski angle combined with the crab waist collision scheme. Under these conditions, the luminosity and the beam–beam tune shifts are strongly influenced by the bunch length. On the other hand, in this machine, the beamstrahlung effect is dominant too, leading to an increase of bunch length and energy spread. Moreover, due to the extreme beam parameters, new important beam–beam instabilities have been found, such as the so-called coherent X-Z instability. Finally, the bunch length and energy spread are also affected by collective effects. In this paper, we study the beam–beam interaction, by focusing on the X-Z instability for FCC-ee, in the lowest energy configuration (45.6 GeV, Z-resonance), by taking into account, self-consistently, the combined effects of beamstrahlung and the machine impedance model that has been evaluated so far. Finally, we also discuss some possible mitigation methods.

1 Introduction

The Future Circular Collider (FCC) Study [1] aims at designing hadron and lepton circular colliders able to ensure a worldwide particle physics programme after LHC. The new machines will be placed in an about 100 km tunnel in the CERN region.

Within this project, the lepton machine, called FCC-ee [2], is foreseen to operate in four different stages, each one corresponding to a different beam energy, ranging from 45.6 GeV to 182.5 GeV, covering the Z-resonance, the WW threshold, the HZ production peak and top quark ($t\bar{t}$) pair with unprecedented precision and with luminosities ranging from about 10^{34} to several units of $10^{36} \text{ cm}^{-2} \text{ s}^{-1}$ per collision point (see Table 1).

This work was partially supported by the European Union’s Horizon 2020 research and innovation programme under Grant No 951754—FCCIS Project, by the National Natural Science Foundation of China, Grant No. 11775238, and by INFN National committee V through the ARYA project.

^a e-mail: mauro.migliorati@uniroma1.it (corresponding author)

Table 1 Parameter list used in simulations

	Z	WW	ZH	$\hat{t}\hat{t}$	
Circumference (km)	97.75 km				
Beam energy (GeV)	45.6	80	120	175	182.5
Bunch population (10^{11})	1.7	1.5	1.8	2.2	2.3
Bunches per beam	16640	2000	328	59	48
RF frequency (MHz)	400			400/800	
RF Voltage (GV)	0.1	0.75	2.0	4.0/5.4	4.0/6.9
Energy loss per turn (GeV)	0.036	0.34	1.72	7.8	9.2
Longitudinal damping time (turns)	1273	236	70.3	23.1	20.4
Momentum compaction factor 10^{-6}	14.8		7.3		
Horizontal tune	269.139	269.124	389.129	389.108	
Vertical tune	269.219	269.199	389.199	389.175	
Synchrotron tune	0.025	0.0506	0.0358	0.0818	0.0872
Horizontal emittance (nm)	0.27	0.84	0.63	1.34	1.46
Vertical emittance (pm)	1.0	1.7	1.3	2.7	2.9
IP number	2				
Nominal bunch length (mm) (SR/BS)*	3.5/12.1	3.0/6.0	3.15/5.3	2.01/2.62	1.97/2.54
Nominal energy spread (%) (SR/BS)*	0.038/0.132	0.066/0.131	0.099/0.165	0.144/0.186	0.150/0.192
Piwinski angle (SR/BS)*	8.2/28.5	3.5/7.0	3.4/5.8	0.8/1.1	0.8/1.0
ξ_x/ξ_y	0.004/0.133	0.010/0.113	0.016/0.118	0.097/0.128	0.099/0.126
Horizontal β^* (m)	0.15	0.2	0.3	1.0	
Vertical β^* (mm)	0.8	1.0	1.0	1.6	
Luminosity/IP ($10^{34}/\text{cm}^2\text{s}$)	230	28	8.5	1.8	1.55

*SR: synchrotron radiation, BS: beamstrahlung

A Conceptual Design Report (CDR) of the machine was published in 2019 [2] and now a feasibility study is in progress to deliver, by the end of 2025, input for the next European Particle Physics Strategy Update, expected for 2026-2027.

In Table 1, the parameter list corresponding the four different machine regimes of FCC-ee is shown. The table shows that the beam emittances are very small while the stored beam currents are close to the best values achieved in the last generation of e^+e^- factories. A careful study of collective effects is then necessary to guarantee the required machine performances and avoid beam instabilities. In this paper, we will focus our attention on the Z-resonance configuration since it is the most critical to collective effects and instabilities because of the lowest beam energy combined to the highest beam current, the lowest emittances and the longest damping times.

In the future electron-positron super-colliders such as FCC-ee and CEPC [3], the high luminosity will be achieved by exploiting the so-called crab waist collision scheme with a large Piwinski angle [4,5], defined as

$$\Phi = \frac{\sigma_z}{\sigma_x} \tan\left(\frac{\theta}{2}\right), \quad (1)$$

with σ_x the horizontal rms size at the interaction point, σ_z the rms bunch length and θ the crossing angle.

Differently from the past generation of colliders, the longitudinal beam dynamics becomes more important in reaching the design luminosity goals of these machines. In particular, with a very large Piwinski angle, both the luminosity and the beam–beam vertical tune shift scale inversely to the bunch length while the beam–beam horizontal one decreases proportionally to the second power of the bunch length according to the following scaling laws [6]

$$L \propto \frac{N\xi_y}{\beta_y^*}, \quad \xi_y \propto \frac{N\sqrt{\beta_y^*/\varepsilon_y}}{\sigma_z\theta}, \quad \xi_x \propto \frac{N}{(\sigma_z\theta)^2}, \quad (2)$$

where L is the luminosity, N the bunch population, $\xi_{x/y}$ the betatron tune shifts due to the beam–beam effect, β^* the beta function at the interaction point and ε_y the vertical beam emittance.

In addition, for the future colliders with their extreme beam parameters, several new effects can take place in collision, such as beamstrahlung [7], coherent X-Z instability [8–10] and 3D flip-flop [11]. The longitudinal beam dynamics plays an essential role for these effects.

In particular, the X-Z instability, which is the main topic of this paper, is characterised by the horizontal bunch oscillations along the bunch length and respective horizontal emittance growth. As it has been shown in [12] for CEPC, the interplay between beam–beam interaction, beamstrahlung and the longitudinal beam coupling impedance may affect both the X-Z instability and the beam parameters in the stable betatron tune areas. It has been observed in numerical simulations that the stable areas get narrower and their positions on the betatron tune diagram are shifted because of the impedance-related synchrotron tune reduction. On the other hand, the horizontal beam blow-up becomes somewhat weaker due to the synchrotron frequency spread induced by the impedance.

In turn, for the betatron tunes inside the stable areas, the bunch length slightly increases and the energy spread decreases due to the combined effects of beamstrahlung and coupling impedance. It has been also observed that the longitudinal microwave instability is suppressed in collision [13]. Indeed, the beamstrahlung results in both a larger energy spread and longer bunch length, thus providing the microwave instability suppression, also according to the Boussard criterion [14].

The first simulations of the combined effect of beamstrahlung and longitudinal impedance for the CEPC [15] have revealed that there were no good working points free of the X-Z instability for the parameters reported in the CEPC CDR [3]. In order to mitigate the instability, it has been decided to reduce the horizontal beta function at the interaction point, as discussed in Ref. [12].

Considering the importance of the interplay between beam–beam interaction, beamstrahlung and the beam coupling impedance, we have undertaken careful studies for the FCC-ee collider. Section 2 of this paper discusses the impedance model evaluated so far, while in Sect. 3 we report the longitudinal impedance-related collective effects without beam–beam collisions. 3D self-consistent simulations taking into account the combined effect of beam–beam and coupling impedance are studied in Sect. 4. The results for this machine configuration clearly show that, with the impedance model evaluated so far, there are no good working points where the FCC-ee design luminosity can be achieved with the current CDR parameters. In order to overcome harmful consequences of the instabilities, in Sect. 5 we propose possible mitigation solutions. The advantages and disadvantages of the techniques are then discussed. Concluding remarks are finally summarised in Sect. 6.

2 Impedance model

Due to the fact that FCC-ee is an ongoing project and that a technical design report does not exist at the moment, the machine impedance model still represents a work in progress. Indeed, for several devices, as, for example, the collimators and injection kickers, a design has not been defined yet. Moreover, for some other devices, refined models for the determination of the coupling impedance are planned in the future. As a consequence, we report here some important contributions that have been evaluated so far and that already demonstrate how this machine can become critical due to collective effects. On the other hand, an advantage of a machine still in the design status is that it is possible to interact with other groups, such as, vacuum and instrumentation, in order to find optimal solutions to minimise the impact of a device on the total machine impedance budget.

Here, we focus our attention only on the longitudinal plane. Moreover, since the nominal (minimum) bunch length at zero intensity without collision is 3.5 mm, as shown in Table 1, corresponding to a beam spectrum cut-off frequency of about 13.6 GHz, we considered, for the impedance evaluation, a maximum frequency of 50 GHz, where the amplitude of the beam spectrum is negligible.

For what concerns the wakefields, electromagnetic 3D simulators, such as CST Microwave Studio [16], which we have used for the electromagnetic characterisation of several devices, can give in output the wake potential of a bunch, but not the Green function of a point charge that should be ideally used in beam dynamics simulation codes. As a consequence, in order to simulate the collective effects, for each device we have evaluated the wake potential of a 0.4 mm Gaussian bunch, much shorter than the nominal bunch length. As a check if this could be considered a good candidate as Green function, we have then convoluted this wake potential with the 3.5 mm Gaussian bunch distribution, and compared the results with a second electromagnetic simulation using directly the nominal bunch length of 3.5 mm.

As already discussed in [17, 18], the most important contribution to the total machine impedance is represented by the resistive wall. The beam vacuum chamber has a circular profile with a radius of 35 mm with two small lateral winglets of 9 mm height needed to place synchrotron radiation absorbers. Since they represent a small perturbation to the machine impedance, in this paper we have neglected them. The model of the circular beam pipe considered for the evaluation of the coupling impedance, shown in Fig. 1, is supposed to be made of copper with a thickness of 2 mm having a NEG coating of 100 nm. Behind the copper, we supposed to have a 6 mm of dielectric (air) and then an infinite layer of iron. The wakefield and the coupling impedance due to the resistive wall have been calculated by using the code IW2D [19], which takes into account multilayer systems, and they are shown

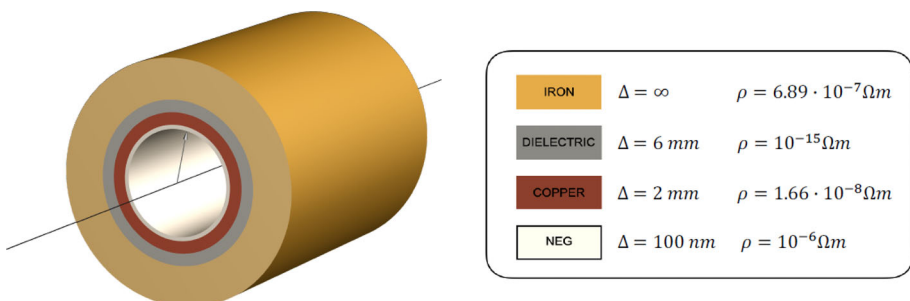


Fig. 1 Model of the vacuum chamber with the four simulated layers

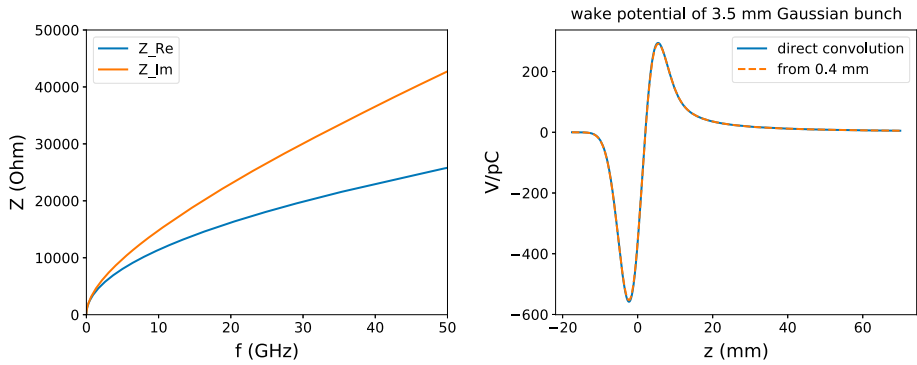


Fig. 2 Left: real and imaginary part of the resistive wall impedance. Right: resistive wall wake potential of a 3.5 mm Gaussian bunch obtained as convolution by using the wakefield (blue curve) and the wake potential of a 0.4 mm Gaussian bunch (orange line)

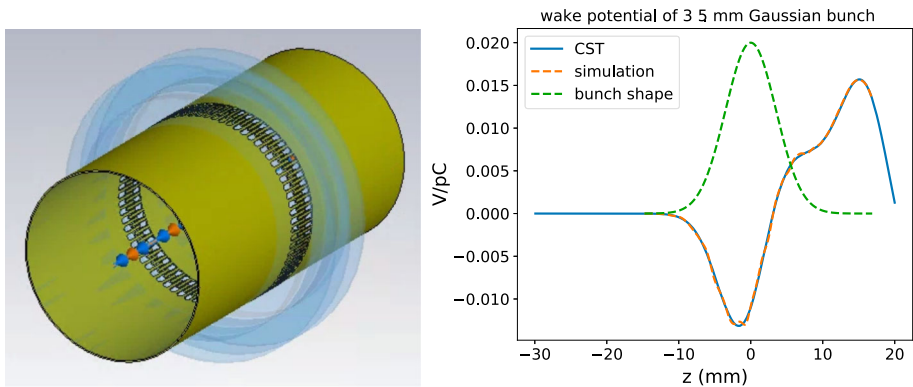


Fig. 3 CST model of the bellows (left) and wake potential of 3.5 mm Gaussian bunch obtained directly by CST (blue curve) and with the convolution by using the wake potential of a 0.4 mm Gaussian bunch

in Fig. 2. In the left-hand side of the figure, the real and imaginary parts of the longitudinal impedance are shown. As demonstrated in [17], the excess of the imaginary part with respect to the real one is essentially due to the thin coating. This difference is proportional to the coating thickness and, in principle, could be reduced by decreasing it.

For this contribution, the wakefield of a point charge is given directly by IW2D as Fourier transform of the impedance. However, for self-consistency with the other contributions obtained with CST, also in this case we have evaluated the wake potential of a 0.4 mm Gaussian bunch as Green function to be used in simulations, and, as a check, convoluted it with the nominal bunch length and compared the result with the wake potential obtained directly from the convolution of the wakefield with the 3.5 mm Gaussian bunch. In the right-hand side of Fig. 2, a comparison between the two methods shows an excellent agreement.

Another important contribution to the machine impedance is represented by the bellows with RF fingers necessary to guarantee electric contacts between the two parts of the beam pipe. Simulations of the device are quite complex due to the small mesh size necessary to model the tiny contacts visible on the left-hand side of Fig. 3. On the right-hand side of the same figure, we have reported the wake potential of a 3.5 mm Gaussian bunch as given directly by CST and the one reconstructed from the convolution by using a wake potential

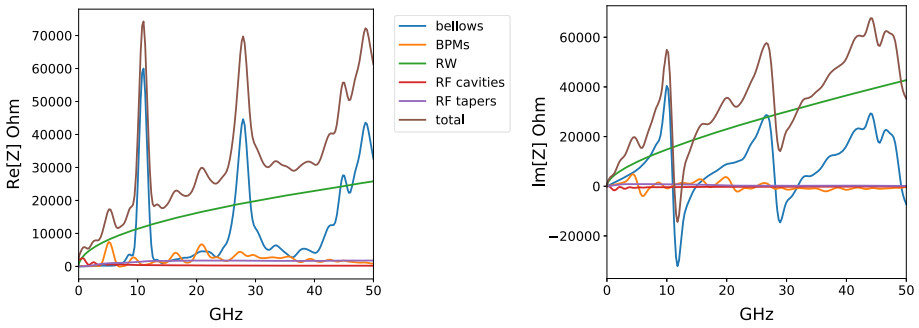


Fig. 4 Real (left) and imaginary (right) part of impedance of different devices. The total impedance is the sum of all the contributions

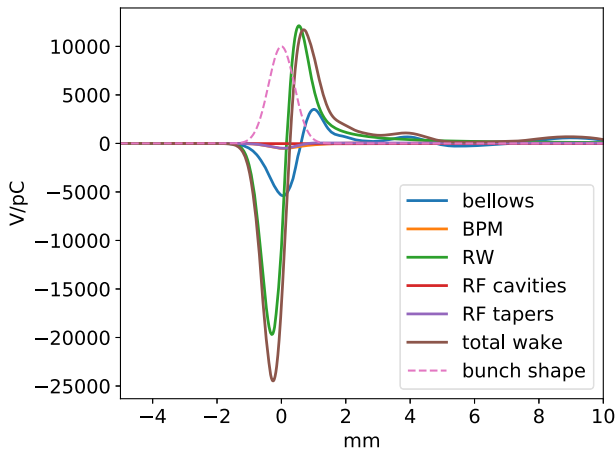


Fig. 5 Wake potential of a 0.4 mm Gaussian bunch due to different devices and used as input for beam dynamics simulations

of a 0.4 mm Gaussian bunch. Also in this case, we have an excellent agreement. For the total contribution to the impedance budget, we have considered 20000 devices distributed all along the machine.

In addition to resistive wall and bellows, we have also evaluated the contribution due to the 400 MHz RF system, made by 52 single cell cavities arranged in groups of 4 for each cryomodule, which has, at each end, a taper 500 mm long, which guarantees a transition from 50 to 150 mm circular pipe inside the cryomodule. Finally, also 4000 BPMs have been taken into account. The total impedance, as well as the contribution of each device, is shown in Fig. 4, while the wake potential of the 0.4 mm Gaussian bunch, used as Green function in the simulation code and also in the convolution product to determine the wake potentials of 3.5 mm bunch of Figs. 2 and 3 is shown in Fig. 5. Both figures confirm the importance of resistive wall and bellows which represent the main sources of the machine impedance.

In Table 2, we have summarised the number of elements for each device evaluated so far together with the corresponding loss factors at the two nominal bunch lengths of 3.5 mm and 12.1 mm.

Table 2 Number of elements and loss factors (k_{loss}) of the main FCC-ee components at bunch lengths of 3.5 mm and 12.1 mm, in the lowest energy case of 45.6 GeV

Component	Number	k_{loss} 3.5 mm (V/pC)	k_{loss} 12.1 mm (V/pC)
Resistive wall	97.75 km	214.9	33.1
Bellows	20000	129.3	0.94
BPMs	4000	40.1	4.81
RF cavities	52	17.0	8.76
RF double tapers	13	25.4	2.33
Total		426.7	49.94

3 Impedance induced collective effects

In this section, we start discussing the collective effects by considering the longitudinal beam dynamics of a single bunch without beam–beam effects. It is known from theory and measurements that at low intensity the wakefields induce a potential well distortion [20,21], which increases bunch length and changes the Gaussian distribution of the bunch, maintaining constant the energy spread [22]. However, above a given intensity threshold, also the energy spread starts to increase in what is known as microwave instability regime, characterised by a turbulent behaviour of the longitudinal phase space [23].

Single bunch beam dynamics simulations by taking into account the total longitudinal wake potential of a 0.4 mm Gaussian bunch evaluated so far and shown in Fig. 5 have been performed with the tracking codes PyHEADTAIL [24] and SBSC [25]. These codes use macro-particles, and they slice the bunch distribution in order to evaluate the convolution integral for the determination of the collective effects. With this approach, the number of slices plays an important role. To verify the independence of the results with this number, the codes were benchmarked against another code, MuSiC [26], which uses a completely different approach with respect to the slices, giving a very good agreement.

The beam parameters used in this paper are those summarised in Table 1. Nominal bunch length and energy spread are evaluated at zero bunch population, without taking into account the collective effects. By including the additional radiation due to the beamstrahlung effect in collision, the nominal bunch length and energy spread are much larger, indicating a strong influence of beam–beam on the collective effects.

In Fig. 6, we show the rms energy spread σ_p (top) and bunch length σ_z (bottom) as a function of the bunch population N_p without (red curves) or with beamstrahlung (green curves). The first case corresponds to the regime without collisions, while the second one can be preliminarily thought as the case when the beams are colliding.

We can see from the figure that, without collision, at the nominal intensity of 1.7×10^{11} , we are in the microwave regime, with a bunch length increasing by a factor of about 2.4 with respect to the nominal one, and an energy spread of a factor of about 1.6. Indeed, from the phase space snapshot obtained with the SBSC code and shown in Fig. 7, left-hand side, we can see a strong instability with arms coming out from the core of the distribution. Also the longitudinal bunch shape is strongly distorted from the original Gaussian one, as shown on the right-hand side (bunch head on the left). The bump in the tail of the longitudinal bunch distribution is due to the bottom right arm and it changes in time since the phase space distribution rotates.

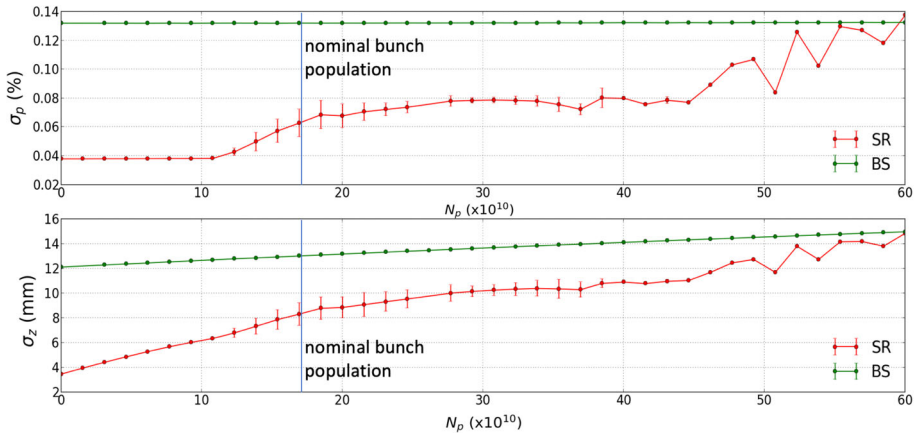


Fig. 6 Energy spread σ_p (top) and bunch length σ_z (bottom) as a function of the bunch population N_p with (BS) and without (SR) beamstrahlung, which is considered here independent of the longitudinal impedance

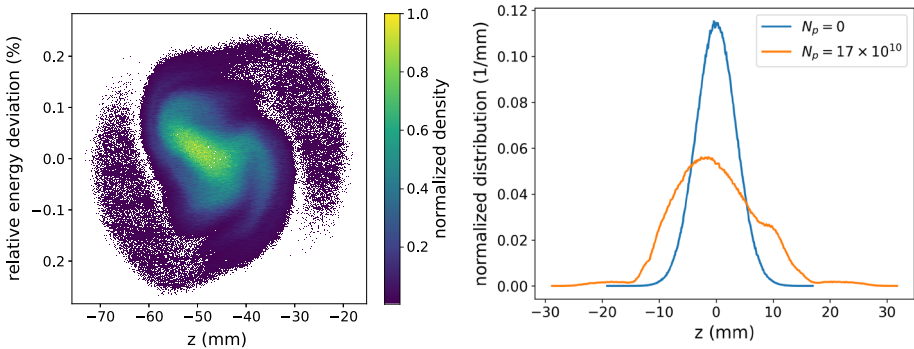


Fig. 7 Longitudinal phase space (left) and bunch distribution (right) snapshots at nominal intensity

On the other hand, in collision, by considering here the beamstrahlung not influenced by the longitudinal wakefields, we can see that the energy spread remains constant up to a bunch population of 6×10^{11} , that is, at the nominal intensity, we are well below the microwave instability threshold and there is only the potential well distortion which slightly increases the bunch length.

It is important to underline that in this analysis we considered the beamstrahlung and the collective effects due to the wakefields independent of each other. In this situation, the increased longitudinal emittance due to beamstrahlung helps to mitigate the effects of wakefields.

However, beam–beam interaction and impedance-related collective phenomena are strongly dependent on each other, and, as it has been shown in [12], a crosstalk between them can result in both positive and harmful effects influencing the beam dynamics and the collider performance. In particular, the coherent X-Z instability [8] is affected by the longitudinal impedance, modifying the areas of stable motion. As a consequence, in the following section, we investigate the impact of the longitudinal impedance on the FCC-ee beam–beam effect.

4 Beam–beam and longitudinal impedance

As it has already been mentioned in the introduction, beam–beam interaction in the future electron–positron circular colliders is essentially three-dimensional since the luminosity and the beam–beam tune shifts strongly depend on the longitudinal bunch length, as shown by Eqs. (1) and (2). Moreover, in order to increase drastically the luminosity, the future machines should collide high intensity bunches with very small transverse dimensions. This combination gives rise to several new effects taking place in collision, such as beamstrahlung [7], coherent X-Z instability [8] and 3D flip-flop [11]. All these effects have been taken into consideration during the conceptual design phase of the future colliders [2, 3]. Later it has been shown, by using a semi-analytical model and numerical simulations [13], that in the stable tune areas, free of the coherent resonances, the bunch becomes longer and the energy spread reduces if the longitudinal beam coupling impedance is included in the beam–beam interaction treatment. In turn, it has also been observed that the longitudinal microwave instability can be suppressed in beam–beam collision.

Among the new effects taking place in collision, the coherent horizontal-longitudinal (X-Z) instability turns out to be the most critical phenomenon for reaching the design collider performance. It is induced by beam–beam interaction with large Piwinski angle and, differently from the normal impedance induced collective instability, it is excited by a very local “wake-force” (horizontal beam–beam force). This new coherent instability also differs from the classic incoherent synchro-betatron resonances excited by the beam–beam interaction. The instability manifests itself as a horizontal beam size variation along the longitudinal bunch length, changing from turn-to-turn similarly to a “snake motion”. The instability severely limits available tunes areas where the design luminosity can be achieved. The semi-analytical scaling law helping to evaluate the threshold of the instability is [11],

$$N_{th} \propto \frac{\alpha_p \sigma_\delta \sigma_z}{\beta_x} \propto \frac{v_s}{\xi_x}. \quad (3)$$

One can understand the physical meaning of the scaling law considering that the coherent synchro-betatron resonances are separated by the synchrotron tune while the strength of the resonances is proportional to the horizontal tunes shift. Since both values depend on the bunch length one can expect that the longitudinal impedance can play an important role in the developing of the instability.

The study of the interplay between beam–beam interaction, beamstrahlung and longitudinal collective effects has been performed with the simulation code IBB [12]. Originally, the code was developed for the study of beam–beam effects in BEPC-II and it has proven to be very reliable in prediction of the luminosity performance of this collider [27]. Indeed, the difference between the simulated luminosity and that measured experimentally does not exceed 10–20%. IBB has been further cross-checked with the strong-strong code BBSS [28] including the beamstrahlung effect [29]. The addition of the longitudinal beam coupling impedance is the new feature of IBB [12]. Differently from the tracking codes discussed in the previous section, IBB uses in input the longitudinal coupling impedance shown in Fig. 4. The wake potential is evaluated by the inverse Fourier transform of the product of the impedance and the bunch spectrum. Finally, the bunch is represented by macroparticles and sliced in the longitudinal direction.

Without collision, the code has been benchmarked against ELEGANT [30] results by simulating the bunch lengthening in CEPC using the impedance model of Ref. [12]. In turn, we have also verified that the collective effects of FCC-ee are simulated correctly by

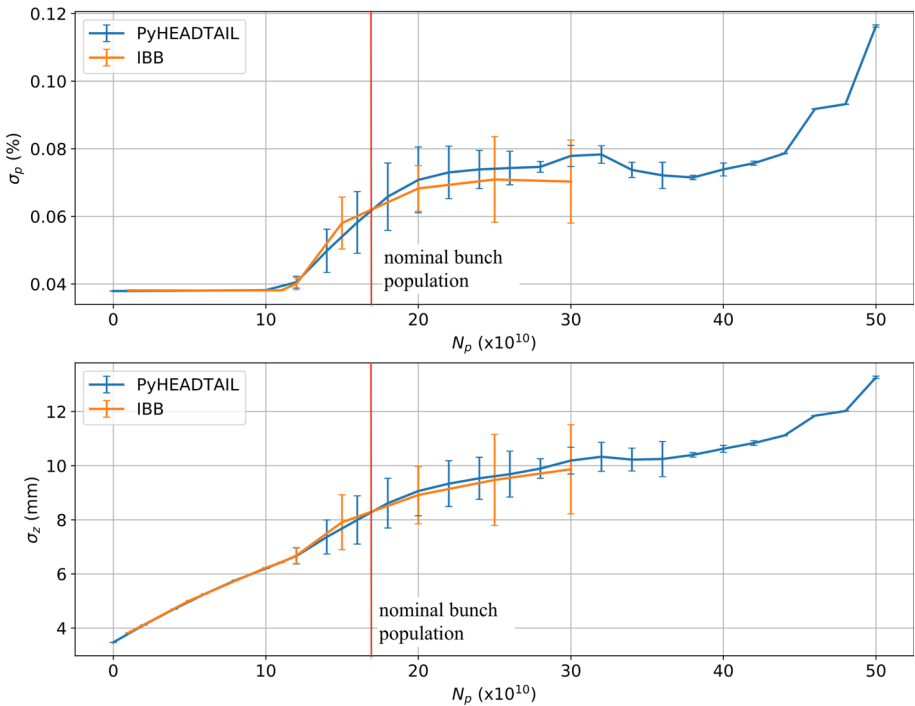


Fig. 8 Comparison between IBB and PyHEADTAIL of energy spread σ_p (top) and bunch length σ_z (bottom) as a function of the bunch population without collision

comparing bunch length and energy spread versus the bunch population between IBB and PyHEADTAIL. In Fig. 8, we can see that the agreement between the two codes is excellent.

In the IBB code, due to the fact that FCC-ee has two interaction points, only half of the machine is simulated, being symmetric the other half. The study of the X-Z instability is performed by evaluating the horizontal beam dimension at different intensities and horizontal tunes. A horizontal blow-up is a manifestation of this instability and the value of beam size is related to its strength.

In Fig. 9, we have reported the results of the beam–beam simulations without the longitudinal coupling impedance at different horizontal tunes and bunch intensities. In particular, the white colour represents the stable region. The colour map in the right hand-side of the figure reports the increase of the horizontal beam size σ_x with respect to the nominal value. Without the collective effects, there is a stable corridor at any simulated intensity up to a bunch population of 1.8×10^{11} with the half horizontal betatron tune $\nu_x/2$ between 0.566 and 0.571. This stable region is, however, strongly reduced when we include the impedance model, as shown in Fig. 10.

The figure clearly shows that, in addition to the fact that we have a narrower stable region at the nominal intensity, we cannot use a fixed betatron tune during the beam filling from scratch (the so-called bootstrapping), but a gymnastic with the quadrupole magnets should be foreseen as a function of the bunch population in order to change the betatron tune which guarantees a stability of the horizontal beam size (white regions) at any intensity. In particular, with a bunch population of about 10^{11} there is a very narrow stable tune between $\nu_x/2 = 0.558$ and 0.559. The X-Z instability is a transverse mode coupling instability, and it would be

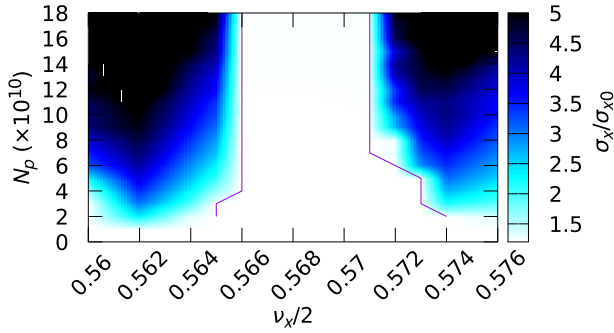


Fig. 9 Blow-up of the horizontal beam size σ_x/σ_{x0} as a function of the bunch population and of the horizontal tune scan without impedance

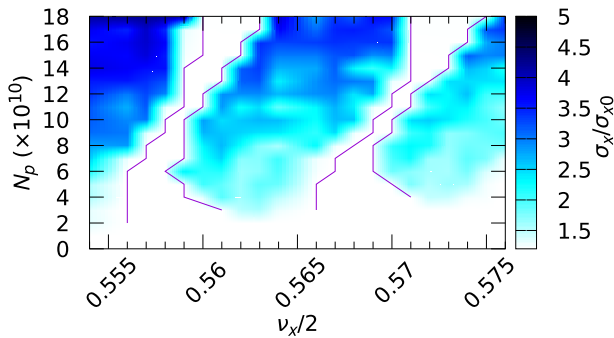


Fig. 10 Blow-up of the horizontal beam size σ_x/σ_{x0} as a function of the bunch population and of the horizontal tune scan by including the impedance

excited when different azimuthal modes are coupled. Since the incoherent synchrotron tune would change with bunch population, the unstable tune area would shift correspondingly. Then, the shift of the stable region versus bunch population could be explained by the change of incoherent synchrotron tune caused by the longitudinal impedance. It is also interesting to note that, in this case, the blow-up is generally weaker due to the synchrotron frequency spread induced by the impedance.

At the nominal bunch intensity of 1.7×10^{11} , if we suppose to be in the small stable region with $\nu_x/2$ between 0.56 and 0.563, the bunch length and the energy spread are very close to those of the parameter list with the inclusion of beamstrahlung, in particular they are about 12.6 mm and 0.126%, as shown in Fig. 11. This result demonstrates that in the stable region the analysis performed in the previous section by including the beamstrahlung as an independent effect is valid and the microwave instability is suppressed. Moreover, it is interesting to observe that bunch length and energy spread are much smaller in the unstable regions because the transverse emittance grows due to the instability so that the beamstrahlung becomes weaker.

The results of the simulations of this section show that there is a strong interplay of the longitudinal coupling impedance with the beam–beam effect that drastically changes, and in particular reduces, the stable regions free from the X-Z instability. On the other hand, if there is no blow-up of the horizontal size, at the nominal bunch intensity the beamstrahlung increases the longitudinal emittance in such a way to suppress the microwave instability.

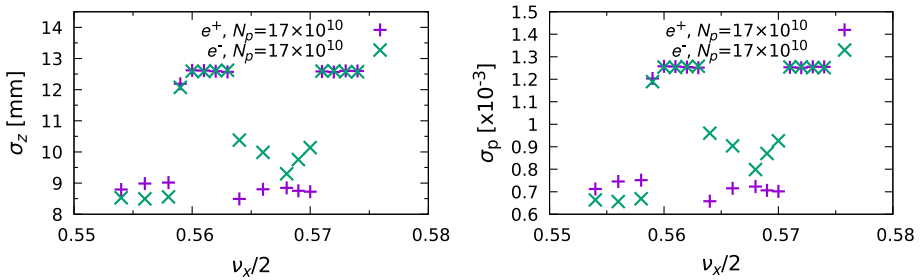


Fig. 11 Bunch length (left) and energy spread (right) at the nominal bunch population as a function of the horizontal betatron tune

If the collision is stable, the luminosity would only reduce by a few percent ($\sim 2\%$) considering the longitudinal impedance, with a little longer bunch length and smaller energy spread with respect to the nominal ones of Table 1.

5 Countermeasures

As discussed in Sect. 2, the design of FCC-ee is still in progress. As a consequence, the machine impedance evaluated so far will certainly increase due to the contribution of other devices and the previous small stable regions found at nominal intensity could become even narrower or they could totally disappear, in addition to the difficulty to reach the nominal bunch intensity due to the necessary variation of the horizontal tune during the beam filling. Therefore, countermeasures to the X-Z and microwave instabilities have been investigated. In particular, we have considered here two possibilities.

5.1 Higher harmonic cavity

One way to suppress the X-Z and, at the same time, the microwave instability is that of using a higher harmonic cavity system that increases the nominal bunch length. Indeed, longer bunches reduce the horizontal beam–beam tune shift, since, from Eq. (2), this quantity scales inversely to the second power of the bunch length, and this effect helps in suppressing the X-Z instability. Moreover, the amplitude of wake potential due to the coupling impedance decreases with the bunch length, so that longer bunches induce less intense collective effects. Indeed the microwave instability is expected to be weaker in presence of the harmonic cavities as it occurs in several synchrotron light sources [31,32].

Another advantage of the harmonic cavities is represented by the reduction of the synchrotron tune ν_s . As a consequence of this, X-Z resonances of the kind $n\nu_x - m\nu_s$, with ν_x the horizontal tune and n and m integer numbers, take place for the same betatron working points with higher order number n . Therefore, a weaker X-Z instability is expected.

Moreover, the harmonic cavities provide a higher synchrotron frequency spread and a larger Landau damping. This may help to counteract not only the observed instability but also of other kinds, for example by providing additional damping to the longitudinal multi-bunch oscillations.

Finally, longer bunches in collision result in a smaller energy spread due to the beam–strahlung effect.

Table 3 Harmonic cavity parameters

RF frequency (MHz)	Voltage (MV)	Phase (°)
400	100	156.1
1200	23.4	− 11.1

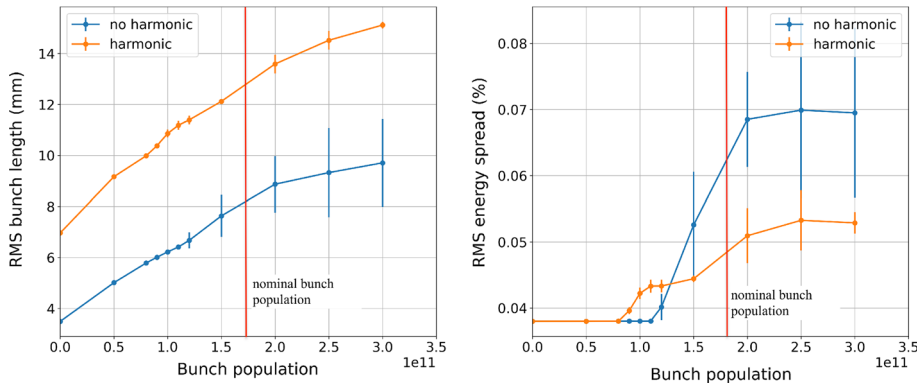


Fig. 12 Bunch length (left) and energy spread (right) versus bunch population with and without the higher harmonic cavity system obtained with the code SBSC without collision

Generally, longer bunches could, in principle, be obtained also by reducing the main RF voltage V_{RF} , since the nominal bunch length is proportional to the square root of V_{RF} . However, the advantage of the harmonic cavities is that longer bunches can be achieved without momentum acceptance reduction.

A possible harmonic cavity configuration is listed in Table 3. In Fig. 12, we show the comparisons of bunch length and energy spread as a function of the bunch population with and without the harmonic cavities, obtained with the code SBSC without collision.

We observe that the bunch length is increased by nearly a factor 2. However, we also observe that the microwave instability threshold is a bit lower, and this could seem surprising. On the other hand, the instability is less strong resulting in a quite lower energy spread at the nominal bunch population with respect to the case without the harmonic cavity system. Indeed, by looking at the normalised spectra of longitudinal bunch distribution momenta, using a similar analysis as that described in Ref. [33], we obtain the results shown in Fig. 13 for some intensities around the microwave instability threshold.

We can see from the figure that at a bunch population of about 1.2×10^{11} , without the harmonic cavity (left-hand side), a line close to the second harmonic of the synchrotron tune appears very strong, suggesting a longitudinal radial mode coupling of the $n = 2$ azimuthal mode. On the other hand, with the harmonic cavity system shown in the right-hand side of the figure, at 9×10^{10} , we observe an unstable line close to $n = 3$, and then, at the higher bunch population of 1.5×10^{11} , even higher azimuthal unstable lines appear. These lines, having higher azimuthal number, correspond to a weaker instability.

The results of the study with harmonic cavity also show that the synchrotron tune, without collision, is reduced by a factor of about 2. Moreover, in collision, due to the increase of energy spread, the lengthening factor generated by the harmonic cavity is smaller so that the final beam–beam horizontal tune shift is only of about $\xi_x = 0.002$, again a factor 2 less with respect to that without the harmonic cavity. That is to say, the ratio of ξ_x/ν_s of Table 1 nearly keeps unchanged in these conditions.

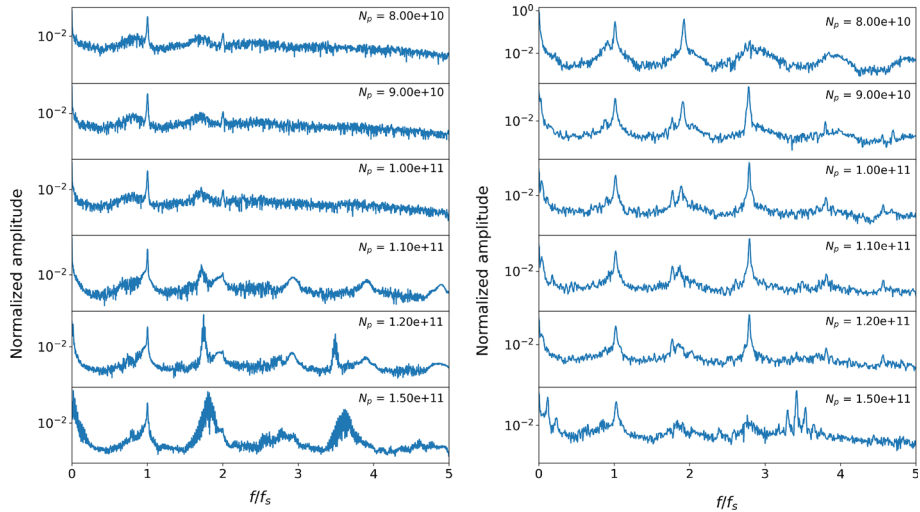


Fig. 13 Frequency spectra of the longitudinal momenta of the bunch distribution at different bunch intensity without (left) and with (right) the higher harmonic cavity

We have performed simulations in collision for three different bunch populations of $N_p = 1.0/1.7/2.0 \times 10^{11}$ in the tune range $0.54 < \nu_x/2 < 0.576$ with a tune step of 0.001, and we have found that, in this case, there is no blow-up of the horizontal beam size in all the scanned intervals, showing that the high harmonic cavity system can really help in suppressing the X-Z instability observed in the previous section. The interesting observation is that, without the inclusion of collective effects, the beam is not always stable, but there are some tune regions presenting horizontal blow-up.

The reason why, in presence of the high harmonic cavity system, collective effects have a mitigation effect on the X-Z instability is supposed to be due to the combined change of some important beam parameters with respect to those of Table 1 corresponding to the CDR configuration [2]: a lower horizontal tune shift $\xi_x = 0.002$, a larger Piwinski angle $\Phi = 39$, a lower half synchrotron tune $\nu_s/2 = 0.005$ and, very important, a different bunch shape.

At nominal intensity, bunch length and energy spread, by including collective effects and beamstrahlung in presence of the harmonic cavity, would be of about 17 mm and 0.083%, respectively, as shown in Fig. 14. These values are larger than those obtained without collision and shown in Fig. 12. The consequence is that now, thanks to collision, bunch length and energy spread behave smoothly in time, without any trace of microwave instability. However, the longer bunch length would produce a luminosity loss from 230 to $200 \times 10^{34} \text{ cm}^{-2} \text{ s}^{-1}$ if we keep the bunch population unchanged. The luminosity can be restored to $230 \times 10^{34} \text{ cm}^{-2} \text{ s}^{-1}$ if the bunch population increases to 2.0×10^{11} and the beam SR power keeps unchanged, with bunch length and energy spread of 18 mm and 0.092%, respectively.

Even if the presence of the harmonic cavity suppresses the X-Z instability in collision with the inclusion of collective effects, showing that this could represent an effective mitigation tool, it is important to underline that we have simulated here the coupling impedance evaluated so far taking into account some devices, but this impedance will surely increase with other contributions, so that another mitigation tool has been investigated.

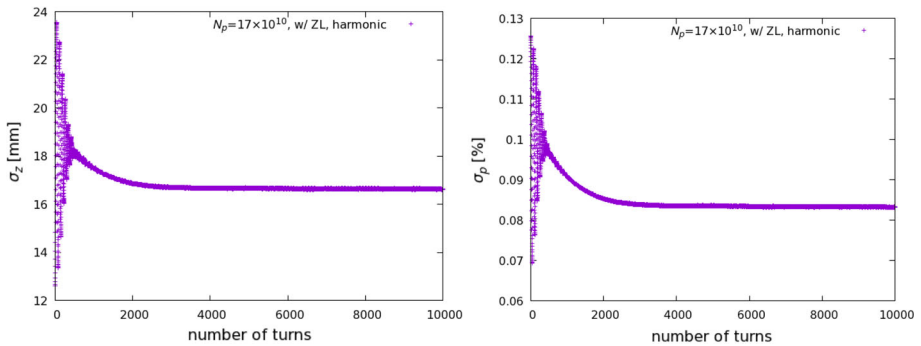


Fig. 14 Bunch length (left) and energy spread (right) evolution during collision with harmonic cavity at design bunch population

Table 4 Machine Parameters of large momentum compaction factor

$\alpha_p [10^{-5}]$	$\epsilon_x [nm]$	$\epsilon_y [pm]$	RF voltage [MV]	$\sigma_{z0} [mm]$
2.5	0.6	1.5	100	4.5

Despite the very positive effect of the higher harmonic cavity system, we have also to remember that there are some issues that should be carefully investigated, such that the transient beam loading in the multi-bunch regime, the additional impedance contribution due to the harmonic cavities, the problem of energy calibration because of the lower synchrotron frequency and its influence on the transverse mode coupling instability, that could represent another critical limitation to the machine performance.

5.2 Higher momentum compaction factor

In order to enlarge the width of safe tune areas represented in Fig. 10, another possible option is to increase the synchrotron tune ν_s while keeping horizontal beam-beam tune shift ξ_x unchanged. This would increase the distance of synchro-betatron resonant lines and, therefore, the stability regions. For this purpose, a larger momentum compaction factor has been proposed by reducing the FODO cell lattice from the original 60/60° to 45/45° [34]. The other parameters used in simulations are shown in Table 4.

Bunch length and energy spread without collision due to collective effects are shown in Fig. 15 compared with those having nominal parameters. We observe that, with higher momentum compaction factor, the microwave instability threshold is just slightly changed. Indeed, by performing the analysis of the normalised spectra of bunch distribution momenta, similar to that of the higher harmonic cavity of the previous section, we obtain very similar plots of Fig. 13 left-hand side, just slightly shifted to a bit higher intensity. Moreover, in this case, in order to reach the nominal luminosity, the bunch population must be higher, so that, from the microwave instability point of view, we should conclude that there is not much gain in increasing the momentum compaction factor.

However, as for the higher harmonic cavity system, also with the higher momentum compaction factor, even if we must operate at higher intensity, the microwave instability is weaker. Another advantage in this case is the larger synchrotron tune which should have a beneficial effect on the transverse mode coupling instability threshold, as well as on the energy

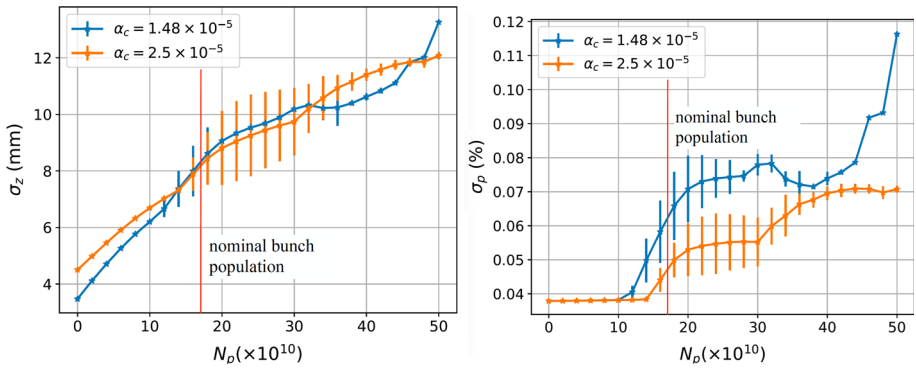


Fig. 15 Bunch length (left) and energy spread (right) versus bunch population with two different momentum compaction factors

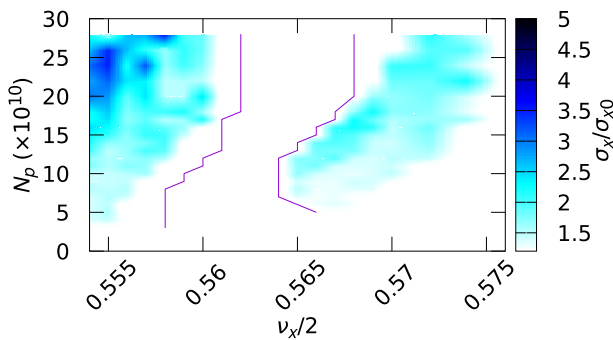


Fig. 16 Blow-up of the horizontal beam size σ_x/σ_{x0} as a function of the bunch population and of the horizontal tune scan for arc cell of $45^\circ/45^\circ$

calibration, even if it could excite lower order X-Z resonances. Moreover, by increasing the nominal bunch population, we can reduce the number of bunches per beam, resulting in a larger bunch separation that helps mitigating the e-cloud effect and ion trapping [35,36].

If we take into account the beamstrahlung and collective effects in collision, we obtain the horizontal beam size blow-up shown in Fig. 16. If we compare it with Fig. 10, we observe that the safe tune areas are much larger and less current dependent, and the horizontal size blow-up is much lower for the tunes affected by the X-Z instability. Even if we increase the bunch population up to $N_p = 2.8 \times 10^{11}$, we find that the X-Z instability is suppressed in a horizontal tune region with width of about 0.004–0.005, not as large as that obtained with the higher harmonic cavity system, but anyway very good from the machine operation point of view. By maintaining the same synchrotron radiation power, the total luminosity is $210 \times 10^{34} \text{ cm}^{-2} \text{ s}^{-1}$ for a bunch population 1.7×10^{11} , and we can restore the CDR value of $230 \times 10^{34} \text{ cm}^{-2} \text{ s}^{-1}$ with the higher bunch population of 28×10^{11} , as shown in Fig. 17. With these two intensities, the bunch length and energy spread in collision, by including collective effects, are equal to 12.2 mm, 0.092% and 15.9 mm, 0.123%, respectively.

Finally, we also observe that for the higher bunch population, the number of bunches is reduced to 10102 with respect to the original 16640 of the CDR (see Table 1).

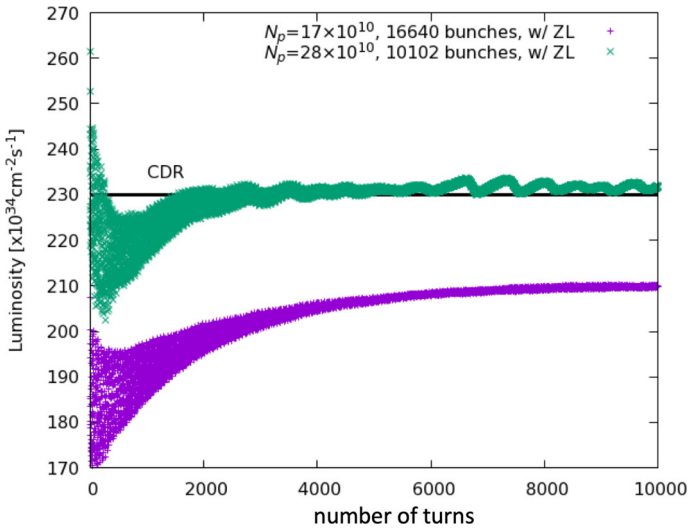


Fig. 17 Luminosity evolution for arc cell of $45^\circ/45^\circ$ by including collective effects

6 Conclusions

Our studies of the interplay between beam–beam interaction and the longitudinal beam coupling impedance for the FCC-ee collider have revealed that this effect can drastically affect the machine performance. Including the impedance in beam–beam simulations, as done in [12] for CEPC machine, indicates a substantial reduction of the “safe” horizontal betatron tune areas, free of the coherent X-Z beam–beam instability, where the design luminosity can be achieved. In addition, the locations of these narrow good regions are shifted on the tune diagram when increasing the intensity of colliding bunches.

Since the impedance is expected to increase adding more components during the vacuum chamber design, the situation could get out of control. That is why we have undertaken studies of eventual mitigation techniques. In particular, we show that the use of harmonic cavities can help suppressing the X-Z instability. The simulations including the 3rd harmonic cavities have demonstrated that there is no instability for the tune range of interest for all the considered bunch intensities. However, it should be kept in mind that the harmonic cavities can have an impact on other beam dynamics aspects such as the transient beam loading in the multi-bunch regime, transverse mode coupling instability and energy calibration. Moreover, the cavities themselves are an additional source of the coupling impedance. All these issues need to be carefully studied.

In our opinion, an application of the collider lattice with a higher momentum compaction factor is even a better solution to the problem. Our simulations of the longitudinal beam dynamics alone show that the microwave instability becomes weaker and in collision the good tune areas are wide enough even for higher bunch intensity. In particular, with a momentum compaction factor of 2.5×10^{-5} , the design luminosity can be achieved with a reduced number of bunches (10102 instead of 16640) by increasing the bunch intensity up to 2.8×10^{11} particles per bunch. In addition, with the increased separation between bunches one can expect a weakening of the electron cloud effects and also of trapped and fast ion instabilities.

Now the work is in progress to update the beam impedance model in accordance with the vacuum chamber design evolution. It is also in our plans to incorporate the transverse beam coupling impedance in a 3D self-consistent beam–beam simulations.

Data availability Data sharing not applicable to this article as no datasets were generated or analysed during the current study.

References

1. <https://fcc.web.cern.ch/Pages/default.aspx>
2. A. Abada et al., FCC-ee: the Lepton Collider: Future Circular Collider Conceptual Design Report. Eur. Phys. J. Spec. Top. **228**(2), 261–623 (2019)
3. CEPC Study Group, CEPC Conceptual Design Report. Volume 1–Accelerator. [arXiv:1809.00285](https://arxiv.org/abs/1809.00285) (2018)
4. P. Raimondi, D. Shatilov, M. Zobov, Beam-beam issues for colliding schemes with large Piwinski angle and crabbed waist. [arXiv:physics/0702033](https://arxiv.org/abs/physics/0702033) (2007)
5. M. Zobov et al., Test of crab-waist collisions at DAFNE Phi factory. Phys. Rev. Lett. **104**, 174801 (2010)
6. D. Shatilov, M. Zobov, Beam-beam collisions with an arbitrary crossing angle: analytical tune shifts, tracking algorithm without Lorentz boost, crab-crossing. ICFA Beam Dyn. Newslett. **37**, 99–109 (2005)
7. V. Telnov, Restriction on the energy and luminosity of e-e+ storage rings due to beamstrahlung. Phys. Rev. Lett. **110**, 114801 (2013)
8. K. Ohmi et al., Coherent beam–beam instability in collisions with a large crossing angle. Phys. Rev. Lett. **119**, 134801 (2017)
9. N. Kuroo, K. Hirose, K. Ohmi, K. Oide, D. Zhou, F. Zimmermann, Mode coupling theory in collisions with a large crossing angle, in *9th International Particle Accelerator Conference*, THPAF089 (2018). <https://doi.org/10.18429/JACoW-IPAC2018-THPAF089>
10. N. Kuroo, K. Ohmi, K. Oide, D. Zhou, F. Zimmermann, Cross-wake force and correlated head-tail instability in beam-beam collisions with a large crossing angle. Phys. Rev. Accel. Beams **21**, 031002 (2018). <https://doi.org/10.1103/PhysRevAccelBeams.21.031002>
11. D. Shatilov, FCC-ee parameter optimization. ICFA Beam Dyn. Newslett. **72**, 30–41 (2017)
12. Y. Zhang, N. Wang, C. Lin, D. Wang, C. Yu, K. Ohmi, M. Zobov, Self-consistent simulations of beam-beam interaction in future e+ e- circular colliders including beamstrahlung and longitudinal coupling impedance. Phys. Rev. Accel. Beams **23**, 104402 (2020)
13. D. Leshehok, S. Nikitin, Y. Zhang, M. Zobov, Combined influence of beamstrahlung and coupling impedance on beam energy spread and length in future lepton colliders. Phys. Rev. Accel. Beams **23**, 101003 (2020)
14. D. Boussard, *Observation of microwave longitudinal instabilities in the CPS, CERN-LabII-RF-INT-75-2* (CERN, Geneva, 1975)
15. N. Wang et al., Mitigation of coherent beam instabilities in CEPC. CERN Yellow Rep. Conf. Proc. **9**, 286–290 (2020)
16. <https://www.3ds.com/products-services/simulia/products/cst-studio-suite>
17. M. Migliorati, E. Belli, M. Zobov, Impact of the resistive wall impedance on beam dynamics in the future circular e+e- collider. Phys. Rev. Accel. Beams **21**, 041001 (2018)
18. E. Belli, P.C. Pinto, G. Rumolo, A. Sapountzis, T. Sinkovits, M. Taborelli, B. Spataro, M. Zobov, G. Castorina, M. Migliorati, Electron cloud buildup and impedance effects on beam dynamics in the future circular e+e- collider and experimental characterization of thin TiZrV vacuum chamber coatings. Phys. Rev. Accel. Beams **21**, 111002 (2018)
19. N. Mounet, *The LHC Transverse Coupled Bunch Instability*. Ph.D. thesis, École Polytechnique Fédérale de Lausanne, Lausanne, Switzerland (2012)
20. A.W. Chao, *Physics of Collective Beam Instabilities in High Energy Accelerators* (Wiley, New York, 1993)
21. K.Y. Ng, *Physics of Intensity Dependent Beam Instabilities* (World Scientific, Singapore, 2006)
22. J. Haisinski, Il Nuovo Cimento **18B**(1), 72 (1973)
23. A.W. Chao, M. Tigner, *Handbook of Accelerator Physics and Engineering* (World Scientific Publishing Co. Pte. Ltd, Singapore, 1998)
24. <https://github.com/PyCOMPLETE/PyHEADTAIL>
25. M. Migliorati, S. Persichelli, H. Damerou, S. Gilardoni, S. Hancock, L. Palumbo, Beam-wall interaction in the CERN Proton Synchrotron for the LHC upgrade. Phys. Rev. Accel. Beams **16**, 031001 (2013)

26. M. Migliorati, L. Palumbo, Multibunch and multi-particle simulation code with an alternative approach to wakefield effects. *Phys. Rev. ST Accel. Beams* **18**, 031001 (2015)
27. Y. Zhang, Beam-beam effects in BEPC-II, in *ICFA Mini-Workshop on Beam-Beam Effects in Hadron Colliders*. CERN, Geneva, pp. 37–41 (2013). <https://doi.org/10.5170/CERN-2014-004.37>
28. K. Ohmi, Simulation of beam-beam effects in a circular e+e- collider. *Phys. Rev. E* **62**, 7287 (2000)
29. K. Ohmi, private communication
30. ELEGANT. <https://ops.aps.anl.gov/elegant.html>
31. N. Carmignani, J. Jacob, B. Nash, S. White, Harmonic RF System for the ESRF EBS, Proceedings of IPAC2017, Copenhagen, Denmark, pp. 3684–3687 (2017)
32. H.S. Xu, N. Wang, Influences of harmonic cavities on the single-bunch instabilities in electron storage rings, in *60th ICFA Advanced Beam Dynamics Workshop on Future Light Sources*, Shanghai, China, pp. 128–132 (2018). <https://doi.org/10.18429/JACoW-FLS2018-WEP2PT024>
33. E. Métral, M. Migliorati, Longitudinal and transverse mode coupling instability: Vlasov solvers and tracking codes. *Phys. Rev. ST Accel. Beams* **23**, 071001 (2020)
34. D. Shatilov, 133th FCC-ee Optics Design Meeting & 4th FCCIS WP2.2 Meeting, ‘Larger Momentum Compaction at Z, as another possible option’ (2021). <https://indico.cern.ch/event/1014189>
35. F. Yaman, Electron Cloud Simulations for FCC-ee Collider Dipoles: Comparisons of SEY Models, Longer Bunch Space and Higher Intensity, 135th FCC-ee optics meeting. <https://indico.cern.ch/event/1017226>
36. L. Mether, Modeling of fast Beam-Ion Instabilities, CERN Yellow Rep. Conf. Proc. 1, 63–68 (2018). <https://doi.org/10.23732/CYRCP-2018-001.63>